The Journal of Experimental Biology 204, 367–378 (2001)
Printed in Great Britain © The Company of Biologists Limited 2001
JEB3135

CHLORIDE CHANNELS IN APICAL MEMBRANE PATCHES OF STELLATE CELLS OF MALPIGHIAN TUBULES OF *AEDES AEGYPTI*

KEVIN R. O'CONNOR AND KLAUS W. BEYENBACH*
Department of Biomedical Sciences, VRT 8014, Cornell University, Ithaca, NY 14853, USA
*Author for correspondence (e-mail: kwb1@cornell.edu)

Accepted 27 October 2000; published on WWW 3 January 2001

Summary

Stellate cells of *Aedes aegypti* Malpighian tubules were investigated using patch-clamp methods to probe the route of transepithelial Cl^- secretion. Two types of Cl^- channel were identified in excised, inside-out apical membrane patches. The first Cl^- channel, type I, had a conductance of 24 pS, an open probability of 0.816±0.067, an open time of 867±114 ms (mean ± S.E.M., four patches) and the selectivity sequence $I^->Cl^- \gg$isethionate>gluconate. The I^-/Cl^- permeability ratio was 1.48, corresponding to Eisenman sequence I. The type I Cl^- channel was blocked by 2,2′-iminodibenzoic acid (DPC) and niflumic acid {2-[3-(trifluoromethyl)anilo]nicotinic acid}. The removal of Ca^{2+} from the Ringer's solution on the cytoplasmic side had no effect on channel activity. The second Cl^- channel, type II, had a conductance of 8 pS, an open probability of 0.066±0.021 and an open time of 7.53±1.46 ms (mean ± S.E.M., four patches). The high density and halide selectivity sequence of the type I Cl^- channel is consistent with a role in transepithelial Cl^- secretion under control conditions, but it remains to be determined whether these Cl^- channels also mediate transepithelial Cl^- secretion under diuretic conditions in the presence of leucokinin.

Key words: Malpighian tubule, stellate cell, patch-clamp, Cl^- channel, mosquito, *Aedes aegypti*.

Introduction

Functionally similar to the kidney, insect Malpighian tubules are involved in ion balance and urine formation. The tubules branch off at the junction of the midgut and hindgut. They are suspended in the hemolymph and produce tubular fluid by transepithelial secretion of solute and water. The yellow fever mosquito *Aedes aegypti* has five Malpighian tubules composed of principal and stellate cells (Beyenbach and Petzel, 1987). In a related species, *Aedes taeniorhynchus*, stellate cells comprise between 16 and 18 % of the cell population (Satmary and Bradley, 1983).

Primary urine is formed by transepithelial secretion of NaCl, KCl and water. Na^+ and K^+ are transported from the hemolymph into the tubule lumen against their electrochemical potentials, indicating active transport powered by ATP-dependent mechanisms in principal cells (Beyenbach, 1994). In contrast, Cl^- moves from the hemolymph into the tubule lumen down its electrochemical potential, indicating passive transport. The route that Cl^- takes across the epithelium is under debate. Although there is good agreement that principal cells do not provide the pathway for Cl^- secretion (Pannabecker et al., 1993; O'Donnell et al., 1996), where and how Cl^- moves across the epithelium from the hemolymph into the tubule lumen is not clear. Our laboratory has evidence supporting a paracellular route through septate junctions in *Aedes aegypti* Malpighian tubules under stimulation with the diuretic peptide leucokinin-VIII (Beyenbach, 1994; Pannabecker et al., 1993). By increasing the Cl^- conductance of the paracellular pathway, leucokinin-VIII increases transepithelial secretion of both NaCl and KCl (Beyenbach, 1994; Pannabecker et al., 1993; Beyenbach et al., 2000). In contrast, O'Donnell and others have evidence for a transcellular route through stellate cells in *Drosophila melanogaster* Malpighian tubules (O'Donnell et al., 1998; O'Donnell and Spring, 2000).

To investigate the possibility of a transcellular pathway for Cl^- secretion in *Aedes aegypti* Malpighian tubules, we explored the apical membrane of *Aedes aegypti* stellate cells using patch-clamp methods. Under control conditions, we observed two types of Cl^- channel that lend support to the view (O'Donnell et al., 1998; O'Donnell and Spring, 2000) of a transcellular pathway for transepithelial Cl^- secretion. Whether these Cl^- channels also mediate transepithelial Cl^- secretion in the presence of leucokinin remains to be elucidated.

Materials and methods

Preparation of Malpighian tubules

Mosquitoes of the species *Aedes aegypti* L. were hatched from eggs and raised to the adult stage (as described by Pannabecker et al., 1993). Female mosquitoes 3–6 days post-

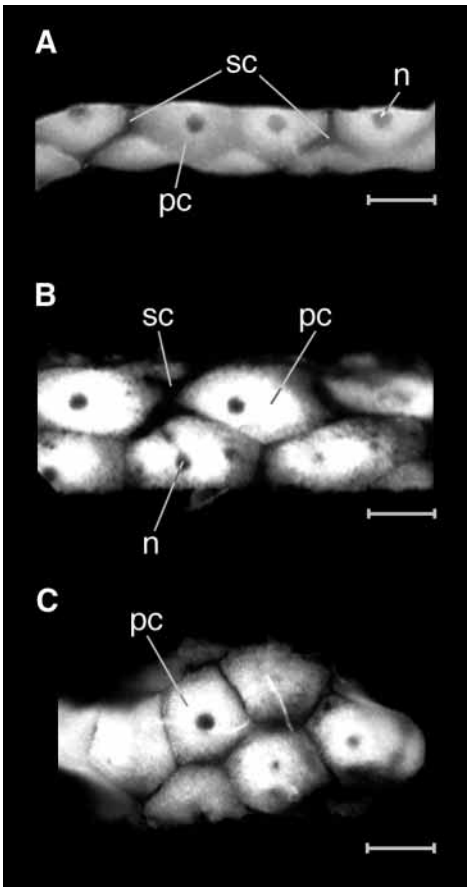

Fig. 1. Photographs of Malpighian tubules of the female yellow fever mosquito *Aedes aegypti*. The tubules are composed of two cell types, principal cells (pc) and stellate cells (sc). The intact tubule is shown in A, revealing the two cell types. Principal cells have a large central nucleus (n). Dissection exposes the apical membrane surface of principal and stellate cells as shown in B and C. Stellate cells are absent from the dissected tubule shown in C. Scale bars, 100 μm.

eclosion were used. On the day of the experiment, the mosquito was cold-anesthetized and decapitated. The gut with Malpighian tubules attached was pulled from the abdominal cavity under Ringer's solution. A Malpighian tubule was removed from its intestinal junction and transferred to a perfusion Ringer bath of volume 0.5 ml. Fig. 1A illustrates a 0.7 mm segment of an intact Malpighian tubule removed from a female mosquito. Whole tubules were approximately 3 mm long and 80 μm wide. When viewed against a dark background, principal cells appear as large, opaque cells with a prominent central nucleus. In contrast, stellate cells are small, thin and transparent (Fig. 1A). A tear or slit was made along the axial length of the tubule using sharp jeweller's broaches to expose the apical (luminal) surface of principal and stellate cells and the junctions between them. Fig. 1B,C shows dissected tubules with the lumen exposed for access by patch pipettes from above. The photographs of Fig. 1 were taken using a CCD-video camera (COHU, model 6410, San Diego, CA, USA) mounted on an inverted microscope (Olympus, model IMT-2, Melville, NY, USA) and fiberoptic illumination.

Electron microscopy

After removal from the abdominal cavity, Malpighian tubules were placed in 0.1 mol l^{-1} sodium cacodylate buffer containing 2.5 % glutaraldehyde (pH 7.4) for 30 min at room temperature (21 °C) and then for an additional 1.5 h at 4 °C. The tubules were treated to three consecutive washes for 10 min in sodium cacodylate buffer at 4 °C before fixation in 2 % osmium tetroxide. After 1 h in osmium tetroxide, the tubules were washed three times in sodium cacodylate buffer at 4 °C. The tubules were subsequently dehydrated stepwise in 10, 30, 50, 70, 90 and 100 % ethanol for 10 min each, and finally dehydrated with 100 % acetone in two 10 min steps. The tubules were gradually infiltrated and imbedded in Epon Araldite, which was cured at 60 °C. The tubules were cut into longitudinal 70 nm sections and examined under a Philips Tecnai 12 Biotwin transmission electron microscope (FEI, Eindhoven, Netherlands).

Chemicals and Ringer's solutions

All chemicals were obtained from Sigma-Aldrich (St Louis, MO, USA). Normal *Aedes* Ringer contained (in mmol l^{-1}): 150 NaCl, 3.4 KCl, 1.0 $MgSO_4$, 1.0 $NaHCO_3$, 1.7 $CaCl_2$, 5.0 glucose and 25.0 Hepes. Low-Cl^- Ringer, to produce a 46-fold Cl^- concentration gradient across excised apical membrane patches of stellate cells, contained (in mmol l^{-1}): 150 $NaC_6H_{11}O_7$ (sodium gluconate) or $NaC_2H_5O_4S$ (sodium isethionate) and 3.4 $KHCO_3$. Ca^{2+}-free Ringer contained the normal Ringer components except that 1.7 mmol l^{-1} $CaCl_2$ was replaced with 3.4 mmol l^{-1} NaCl and 1.0 mmol l^{-1} EGTA was added. In I^- Ringer (Cl^--free), all Cl^- was replaced with I^- except for $CaCl_2$, which was replaced with $CaSO_4$. Cl^- channel blockers were used at a concentration of 0.3 mmol l^{-1}. SITS (4-acetamido-4′-isothiocyanato-stilbene-2,2′-disulfonic acid) and DIDS (4,4′-diisothiocyanato-stilbene-2,2′-disulfonic acid) were dissolved in water before addition to Ringer's solutions, while DPC (2,2′-iminodibenzoic acid) and niflumic acid {2-[3-(trifluoromethyl)anilo]nicotinic acid} were first dissolved in 1 mol l^{-1} NaOH. Prior to use, all Ringer's solutions were titrated to a pH of 7.1 using NaOH. The osmolarity of all Ringer's solutions was approximately 320 mosmol l^{-1}.

Patch-clamp technique

Experiments were conducted at room temperature (21 °C). Patch pipettes were pulled from borosilicate glass capillaries (World Precision Instruments, Sarasota, FL, USA, or Kimble Products, Vineland, NJ, USA) on a vertical puller (Kopf Instruments, model 720, Tujunga, CA, USA) and fire-polished using a heated platinum wire. Pipette resistances were between 5 and 15 MΩ in normal *Aedes* Ringer. Reference and ground electrodes were Ag/AgCl wires. The Ag/AgCl electrode of the Ringer bath was embedded in an agar bridge (4 % in Ringer) to minimize Cl^- junction potentials when the Cl^- concentration in the bath was lowered.

The patch pipette was brought to the apical surface of a stellate cell using an NRC motor-driven micromanipulator system (Newport Corporation, Fountain Valley, CA, USA).

After the formation of a gigaohm seal, patches were excised in the inside-out configuration.

The patch-clamp system consisted of a Grass Medical SD 5 stimulator (Quincy, MA, USA) to measure seal resistance, an Iwatsu SS-5802 digital stereoscope (Japan), a List Medical EPC-7 patch-clamp amplifier and headstage (Darmstadt, Germany), a Bessel filter (Frequency Devices, model 902, Haverhill, MA, USA), an Instrutech VR-10A A/D converter (Elmont, NY, USA), an Axon Instruments Digidata 1200 computer interface (Foster, CA, USA) and a SONY Beta VTR for data storage.

Data analysis

Data were collected and analyzed using Axon Instruments pClamp 6 software (Fetchex, Fetchan, pStat) on a Pentium PC. The acquisition sampling interval was set at 20 μs (50 kHz). Only recordings that displayed distinct channel levels, determined by a large peak separation in the Fetchan all-points histogram, were analyzed. Recordings were filtered at 100 Hz or 500 Hz. In excised membrane patches in the inside-out configuration, Cl^- movement from the pipette to bath is defined as positive current and is represented as an upward deflection in all current traces and current/voltage (*I*/*V* plots). The clamp voltage (V_c) is referenced to ground in the pipette. Accordingly, the clamp voltage indicates the polarity of the cytoplasmic face of the patch. The open probability (P_o) and open time were calculated with pClamp 6 software using data traces of 20 s or greater in duration. Channels were considered to be open if the current level was above a threshold set at 50 % of the maximum open current amplitude. Some patches contained channels with multiple current amplitudes, possibly because of the existence of subconductance states. Data points in *I*/*V* plots were fitted to second-order polynomials.

The data were corrected for voltage offsets resulting from step changes in bath Cl^- concentration by one of two methods. In the first method, the shift in baseline current (seal current) in response to the solution change was calibrated against a shift in baseline current from a known change in clamp voltage (Hayslett et al., 1987). In the second method, we measured the voltage offset *via* a broken patch electrode filled with 3 mol l^{-1} KCl, serving as a free-flowing electrode with no potential in different solutions. Hence, the voltage change observed after a solution change reflected the offset voltage at the agar bridge in the bath. The two methods agreed on offset voltages ranging from 8 to 13 mV when the bath Cl^- concentration was reduced 46-fold.

To describe the current/voltage relationship with a concentration difference for the permeant ion (S) across a barrier, the data were fitted to the Goldman–Hodgkin–Katz (GHK) current equation:

$$I_S = P_S z_S^2 \frac{VF^2}{\boldsymbol{RT}} \times \frac{[S]_i - [S]_o e^{-z_S FV/\boldsymbol{RT}}}{1 - e^{-z_S FV/\boldsymbol{RT}}}, \quad (1)$$

where I_S is the current carried by ion S, z_S is the charge on S, V is the membrane voltage, F is the Faraday constant, $\boldsymbol{R}$ is the gas constant and T is the temperature. P_S is the permeability of ion S in cm s^{-1} (Hille, 1992).

We rearranged the GHK voltage equation according to the experimental conditions to determine the I^-/Cl^- permeability ratio (P_I/P_{Cl}) of the type I channel:

$$\frac{P_I}{P_{Cl}} = \frac{e^{-zFV_{rev}}[Cl^-]_{pipette}}{[I^-]_{bath}}, \quad (2)$$

where V_{rev} is the experimentally determined reversal potential given equal and opposite Cl^- and I^- gradients across the channel.

Results

Electron micrographs

Fig. 2 shows a transmission electron micrograph of a Malpighian tubule of *Aedes aegypti* illustrating both principal

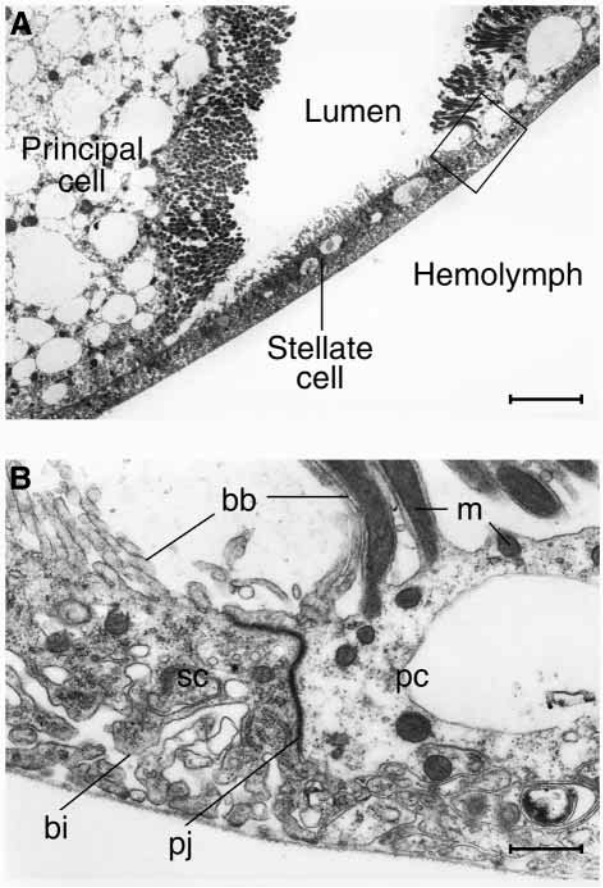

Fig. 2. Transmission electron micrographs of a longitudinal section of an *Aedes aegypti* Malpighian tubule. (A) A stellate cell between two principal cells. Scale bar, 4.4 μm. (B) An enlargement of the outlined region in A. Mitochondria (m) fill the microvillar brush border (bb) of the principal cell (pc); microvilli of the stellate cell (sc) are short, thin and do not contain mitochondria. A thin, convoluted, electron-dense paracellular junction (pj) defines the region of contact between principal and stellate cells. Basolateral infoldings (bi) are also evident in both cell types. Scale bar, 0.6 μm.

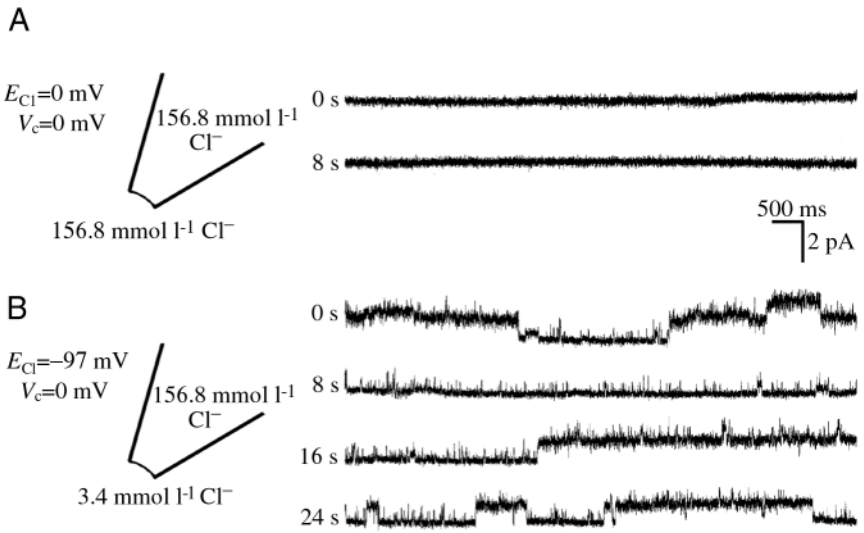

Fig. 3. Representative traces from an excised, inside-out apical membrane patch of a stellate cell of the *Aedes aegypti* Malpighian tubule under two conditions. No channels were observed in the absence of a clamp voltage and a Cl^- concentration difference (A). Reducing the bath Cl^- concentration to 3.4 mmol l^{-1} (isethionate substitution) imposed a 46-fold Cl^- concentration difference across the membrane patch, giving rise to Cl^- current as Cl^- channels open (B). The diffusion of Cl^- from the pipette to the bath through open channels (at 0 mV clamp voltage) is shown as an upward current deflection to multiple current levels, reflecting the usual complexity of channel recordings from the apical membrane of stellate cells. The data were filtered at 500 Hz. E_{Cl}, Cl^- equilibrium potential; V_c, clamp voltage.

and stellate cells. Characteristic features of principal cells include their large size, an abundance of intracellular vesicles and a dense brush border of long slender microvilli filled with mitochondria. The localization of mitochondria in the brush border indicates a region of high metabolic activity at the apical membrane. In contrast, the microvilli of stellate cells are less dense, much shorter and thinner than those of principal cells. Moreover, the microvilli of stellate cells lack mitochondria.

Thin, electron-dense junctions mark the lateral borders of the stellate cell (Fig. 2A). Because of the curvature of the tubule, the cut through this stellate cell has yielded a horizontal section through the left side of the cell and a cross section through the right side. For this reason, the junction appears long on the left side and short on the right side. The different planes of cut are also reflected in the brush border of adjacent principal cells, which appear in both longitudinal and cross section.

Fig. 2B is an enlargement of the rectangle marked in Fig. 2A that illustrates the junctional region between principal and stellate cells in detail. The junction does not have the ladder-like structure characteristic of septate junctions. Accordingly, cellular junctions in *Aedes aegypti* Malpighian tubules may be of the continuous type rather than the septate type (Juan and Carlson, 1994). The basolateral membranes of principal and stellate cells display infoldings. The space between basolateral membrane infoldings appears wider in stellate cells than in principal cells.

Patch-clamp experiments: general considerations

Obtaining high seal resistances of apical membrane patches from stellate cells was frustrated by a success rate of only 3 %. Seal resistances in excess of 10 GΩ were desirable in view of the low conductance of Cl^- channels in apical membrane patches (*vide infra*). However, once a seal had been formed, currents from several Cl^- channels were observed in a majority of patches. The cleanest channel currents were recorded in patches excised from large stellate cells after a gigaohm seal had formed without the use of suction.

Representative traces of excised apical membrane patches of stellate cells are shown in Fig. 3. No channels were observed in

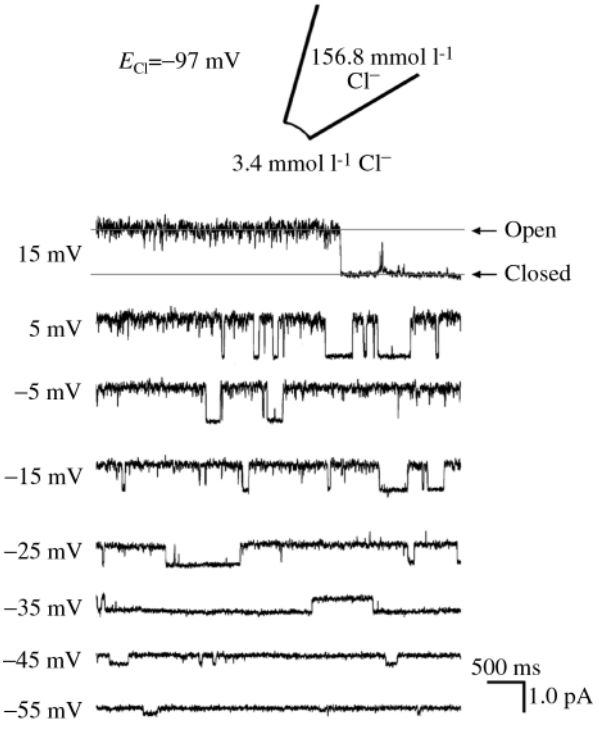

Fig. 4. Representative current recording of the type I Cl^- channel at different clamp voltages. The membrane patch was excised in the inside-out configuration. The Cl^- equilibrium potential (E_{Cl}) was –97 mV (pipette ground) in the presence of a 46-fold Cl^- concentration difference across the patch membrane. Cl^- was replaced by gluconate. Cl^- leaving the pipette through open channels yields an upward deflection in the current trace. The clamp voltage (V_c, referenced to ground in the pipette) is shown to the left of each trace. The data were filtered at 100 Hz.

symmetrical Cl^- and 0 mV clamp voltage (Fig. 3A). The reduction of the bath Cl^- concentration to 3.4 mmol l^{-1} by replacing NaCl with sodium isethionate produced a 46-fold Cl^- gradient, equivalent to a Cl^- equilibrium potential (E_{Cl}) of –97 mV. In the presence of this Cl^- gradient, a multitude of channel open events were observed at 0 mV clamp voltage (Fig. 3B). The variety and complexity of open events under this condition suggests the existence of more than one type of Cl^- channel. From patches that contained a single channel, two distinct types of Cl^- channel were identified on the basis of differences in their open probability, open time and conductance.

Type I Cl⁻ channels: general characteristics

Recordings from a single Cl^- channel, from here on called the type I Cl^- channel, are shown in Fig. 4. The experimental condition is again a 46-fold pipette-to-bath Cl^- concentration difference (gluconate substitution) across the excised patch in the inside-out configuration. As the clamp voltage (V_c) approaches E_{Cl} (–97 mV), the current amplitude decreases, as expected for a Cl^- channel. The representative channel shown in Fig. 4 had a single-channel conductance of 21 pS, an open probability of 0.928±0.034 and an open time of 750±96 ms (means ± S.E.M., N=48 and 60 events, respectively), all measured near 0 mV clamp voltage (±5 mV). In a total of four excised apical membrane patches (with a 46-fold pipette-to-bath Cl^- gradient, gluconate substitution), the type I Cl^- channel had a single-channel conductance of 24 pS, an open probability of 0.816±0.067 and an open time of 867±114 ms (means ± S.E.M.) near 0 mV (±5 mV).

There were no obvious differences in open time and open probability at different clamp voltages. However, 'run-down', i.e. decreased levels of channel activity, was frequently observed over the course of 10–20 min. Multiple type I channels, often five or more, were observed in membrane patches of an estimated 1–2 μm diameter. Pipettes less than 1 μm in tip diameter (approximate surface area less than 0.5 μm^2) were necessary to obtain recordings that contained a single channel.

The large, 46-fold Cl^- concentration difference imposed across the patch membrane did not allows us to follow current through the reversal potential (E_{Cl}), because currents near E_{Cl} were immeasurably small and high clamp voltages jeopardized seal integrity. Nevertheless, Cl^- channels were identified on the basis of current carried by Cl^- diffusion alone (at 0 mV clamp voltage) and extrapolation of the I/V plot to values close to the Cl^- equilibrium potential.

Fig. 5 shows I/V plots for the type I Cl^- channel under three experimental conditions. In the absence of a Cl^- concentration difference across the excised patch (symmetrical Cl^-), the I/V plot is linear with a mean single-channel conductance of 27 pS (Fig. 5A). Data points are means from four apical membrane patches.

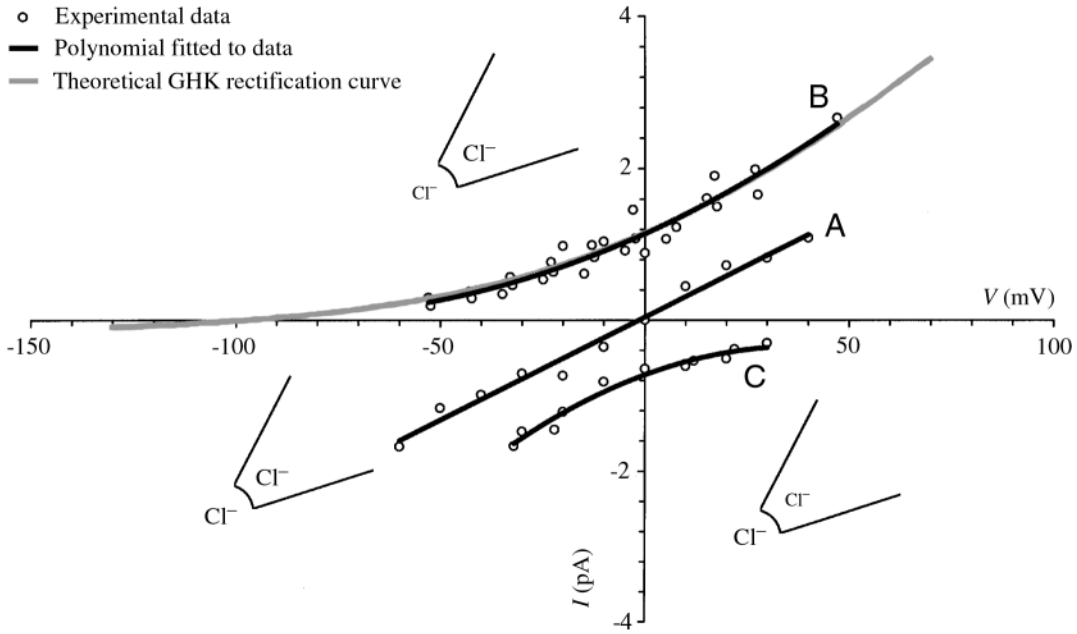

Fig. 5. Current/voltage (I/V) plots for the type I Cl^- channel in three conditions. (A) In symmetrical solutions (control Ringer, 156.8 mmol l^{-1} Cl^-) in both the pipette and bath, the channel exhibited a linear conductance of 27 pS with a reversal potential, V_{rev}, of 0 mV. (B) In the presence of control Ringer (156.8 mmol l^{-1} Cl^-) in the pipette and low-Cl^- Ringer (3.4 mmol l^{-1}) in the bath (gluconate as the substitute anion), the channel exhibited a curvilinear plot with a conductance of 24 pS at 0 mV. Extrapolation of the data yields a V_{rev} approximating the Cl^- equilibrium potential, E_{Cl}, of –97 mV. A plot of the Goldman–Hodgkin–Katz (GHK) current equation (pale line) fits the data, suggesting rectification resulting from Cl^- gradients. (C) Reversed Cl^- gradient. In the presence of control Ringer in the bath (156.8 mmol l^{-1} Cl^-) and low-Cl^- Ringer (3.4 mmol l^{-1}) in the pipette (gluconate as the substitute anion), the channel had a conductance of 20 pS at 0 mV. The data were obtained from apical membrane patches containing only one single channel.

Because the correction for junction potentials in the presence of a 46-fold pipette-to-bath Cl^- concentration difference yielded a range of clamp voltages rather than discrete voltage steps, all data points (rather than means) from four patches are presented in Fig. 5B. Under this condition, the channel has a 24 pS conductance measured at 0 mV. The resultant *I/V* plot reveals outward rectification characteristic of the GHK model. The GHK current equation (equation 1) could be fitted to the experimental data, using the experimental Cl^- concentration gradient ($[Cl^-]_o/[Cl^-]_i$=46) and a Cl^- permeability (P_S) of 7.712×10^{-8} cm s^{-1}.

When the pipette-to-bath Cl^- concentration difference across the patch was reversed such that Cl^- entered the pipette, the type I Cl^- channel exhibited inward rectification (Fig. 5C). Data from three apical membrane patches are pooled to yield a single *I/V* curve withs a 20 pS conductance at 0 mV. In view of the paucity of data, an extrapolation of the *I/V* plot to the reversal potential was not attempted.

At a clamp voltage of 0 mV, the diffusion of Cl^- from the pipette to the Ringer bath carries a current of 1.14 pA (Fig. 5B), whereas diffusion in the opposite direction carries a current of only 0.72 pA (Fig. 5C). Thus, it appears that the type I Cl^- channel displays other mechanisms of rectification in addition to GHK rectification.

Type I Cl^- channel: block

Effects of Cl^- channel blockers were tested from the cytoplasmic side of excised, inside-out apical membrane patches of stellate cells. In these experiments, the patch pipette contained 3.4 mmol l^{-1} Cl^- Ringer (isosmotic Cl^- replacement with gluconate). The bath contained normal Ringer's solution containing 156.8 mmol l^{-1} Cl^- to which Cl^- channel blockers were added or removed by switching bath perfusion lines. Under these experimental conditions, Cl^- and its blocker compete for channel entry from the cytoplasmic side.

Fig. 6 is a representative experiment showing the effects of three Cl^- channel blockers on the activity of the type I Cl^- channel, again at 0 mV clamp voltage. The recording depicted in Fig. 6 differs from those shown in Figs 3 and 4 in that the time axis is compressed in Fig. 6. In addition, the noise level is high because several Cl^- channels are open at the same time. The addition of 0.3 mmol l^{-1} SITS to the Ringer bath had no effect on the current. Similarly, the addition of 0.3 mmol l^{-1} DIDS was ineffective (data not shown). In contrast, the switch from 0.3 mmol l^{-1} SITS to 0.3 mmol l^{-1} niflumic acid caused a gradual reduction in current level and current noise consistent with channel block. Switching the bath Ringer's solution from 0.3 mmol l^{-1} niflumic acid to 0.3 mmol l^{-1} DPC blocked the type I Cl^- channel completely. Channel activity was restored after DPC washout, but in some experiments the effects of DPC lingered for as long as 10 min after washout. Fig. 6 illustrates the effects of three known Cl^- channel blockers tested in sequence on the same patch, and similar results were obtained in four other patches for which each blocker was used alone (data not shown).

The effects of niflumic acid and DPC from the experiment in Fig. 6 are summarized in Fig. 7, where the all-points amplitude histogram (Fetchan) on the right is generated from its corresponding current trace on the left. The current traces are 10 s portions of the experiment in Fig. 6, recorded 1 min after the start of each condition. Fig. 7A is the control period in the absence of channel blockers. Note two observable open levels with high open level noise that reflect the activity of three or four open channels. In the presence of 0.3 mmol l^{-1} niflumic acid (Fig. 7B), the number of open Cl^- channels drops to one or two. There is also a reduction in the open level noise, consistent with a reduction in the number of open channels. In the presence of 0.3 mmol l^{-1} DPC (Fig. 7C), the four channels

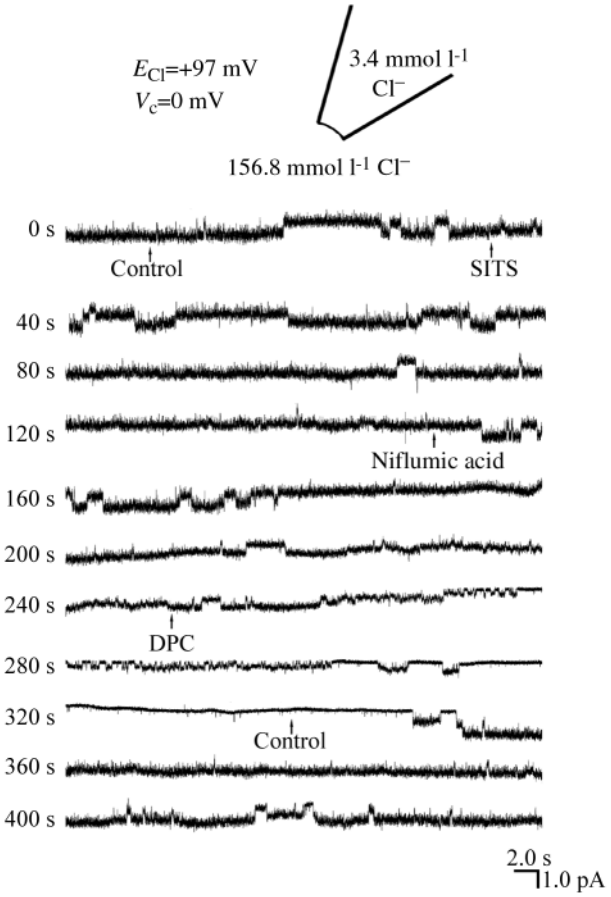

Fig. 6. Block of type I Cl^- channel in an inside-out apical membrane patch of a stellate cell of the *Aedes aegypti* Malpighian tubule. Channel block was studied under conditions of Cl^- diffusion only (0 mV clamp voltage) driven by a 46-fold Cl^- gradient from bath to pipette. Channel openings were observed as downward deflections in the current trace. Arrows mark the addition of SITS, niflumic acid and DPC to the bath, each at a concentration of 0.3 mmol l^{-1}. The control trace depicts total current from several open channels (absence of zero baseline current). The addition of SITS to the bath (the cytoplasmic face of the patch) did not affect channel activity. In contrast, niflumic acid caused a gradual reduction in the number of open channels, and DPC blocked all the channels in the patch. The effects of DPC were reversible with washout. The data were filtered at 100 Hz. E_{Cl}, Cl^- equilibrium potential; V_c, clamp voltage.

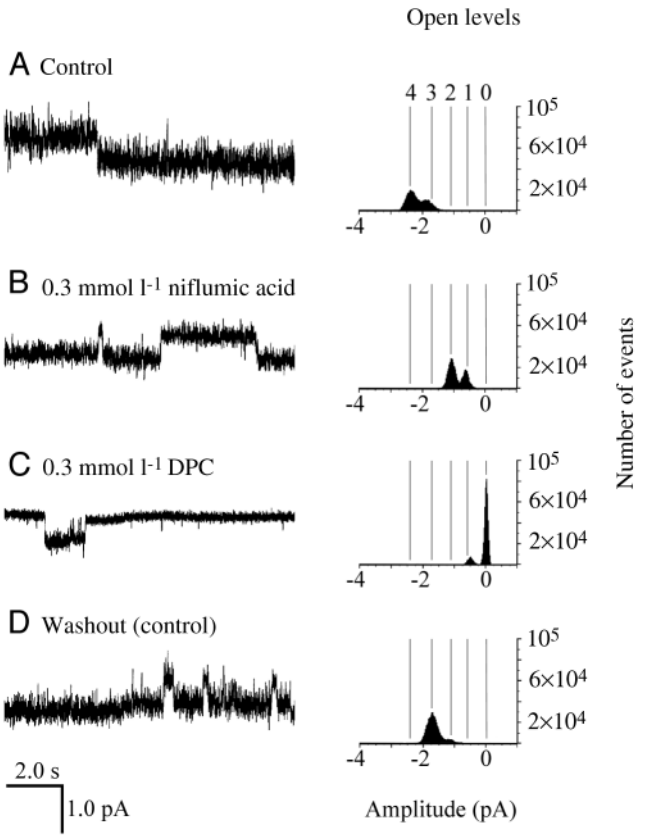

Fig. 7. All-points histogram of the effects of niflumic acid and DPC on the type I Cl^- channel in excised apical membrane patches of stellate cells of *Aedes aegypti* Malpighian tubules. Current traces from Fig. 6 were analyzed for segments of 10 s duration recorded 1 min after the addition of each blocker. Channel openings are downward current deflections, as in Fig. 6. In the absence of channel block (A), the histogram reflects fluctuations between three and four open channels. Niflumic acid reduced the number of open channels to one or two (B). DPC caused a nearly complete channel block (C). Washout of DPC (D) restored channel activity; two or three open channels were observed. The data were filtered at 100 Hz.

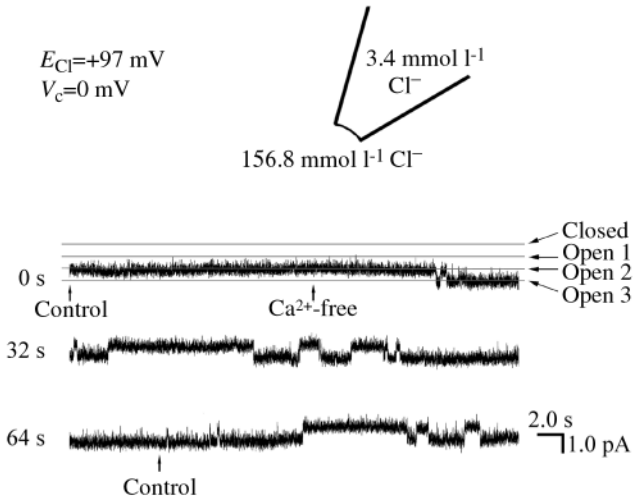

Fig. 8. Continuation of type I Cl^- channel activity in the absence of Ca^{2+}. The current trace reflects the diffusion of Cl^- from bath to pipette through as many as three Cl^- channels at 0 mV clamp voltage. The removal of Ca^{2+} from the Ringer bath (Ca^{2+}-free Ringer plus 1 mmol l^{-1} EGTA) had no effect on channel activity. The data were filtered at 100 Hz. E_{Cl}, Cl^- equilibrium potential; V_c, clamp voltage.

are closed most of the time, except for an occasional opening. Channel openings in the presence of DPC were comparable in current amplitude with control values. Washout of DPC (Fig. 7D) restored the activity of three channels rather than the four channels originally observed.

In several experiments, when the bath solution was changed to establish a 46-fold Cl^- gradient, a high noise level ensued with indistinguishable single channel levels, consistent with the presence of many open channels. Upon application of DPC, the current trace returned to baseline (zero current) as channels closed. By dividing the initial, total current amplitude by the unit current of the type I channel, we could estimate the total number of channels in a patch; there were as many as 12 in one patch.

Type I Cl^- channel: Ca^{2+} insensitivity

To determine whether the activity of the type I Cl^- channel was directly modulated *via* Ca^{2+}, the effect of Ca^{2+}-free Ringer on the cytoplasmic side was of interest. A representative experiment is shown Fig. 8, in which normal Ringer (1.7 mmol l^{-1} Ca^{2+}) on the cytoplasmic side of the patch was replaced with Ca^{2+}-free Ringer (no Ca^{2+} and 1 mmol l^{-1} EGTA), all in the presence of a 46-fold bath-to-pipette Cl^- gradient across the patch (gluconate substitution) at 0 mV clamp voltage. As many as three type I Cl^- channels were active, preventing a drop to baseline current (all channels closed). The removal of Ca^{2+} from the bath (but not from the pipette) had no effect on channel activity. What is shown in Fig. 8 for a single patch experiment was observed in four other patches in which the effects of Ca^{2+} were studied. Prolonged exposure to Ca^{2+}-free Ringer disrupted seal integrity.

Type I Cl^- channel: selectivity

To determine the halide selectivity sequence of type I Cl^- channel, we measured the I^-/Cl^- permeability ratio. This was achieved by imposing equal and opposite Cl^- and I^- diffusion gradients across the path membrane by replacing bath Cl^- (156.8 mmol l^{-1}) with I^-. The *I/V* plot for these experiments is shown in Fig. 9, which depicts mean values from three excised apical membrane patches. Because the pipette contains no I^- and the bath contains no Cl^-, the Nernst potentials for I^- and Cl^- are undefined. Under this condition, the observed V_{rev} still reflects relative permeability. For example, the *I/V* plot for a channel that offers equal permeability to I^- and Cl^- would pass through 0 mV. In contrast, Fig. 9 illustrates a negative current at 0 mV, expected from I^- moving into the pipette rather than Cl^- moving out. Consistent with this interpretation is the reversal potential at approximately +10 mV, indicating a channel more permeable to I^- than to Cl^-. Using this reversal

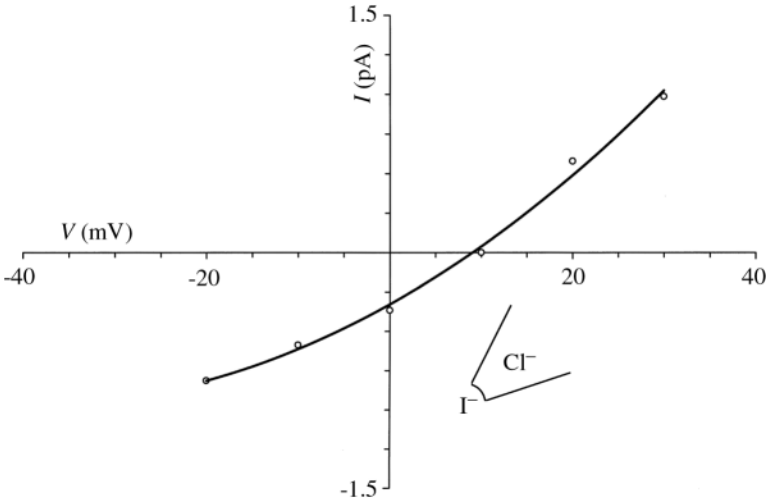

Fig. 9. A current/voltage (*I*/*V*) plot of the anion selectivity of the type I Cl^- channel in excised, inside-out apical membrane patches of stellate cells of *Aedes aegypti* Malpighian tubules. Bath Cl^- (156.8 mmol l^{-1}) was completely replaced with I^- such that the outward Cl^- diffusion gradient was equal to the inward I^- diffusion gradient. A negative current at 0 mV clamp voltage as well as a reversal potential of +10 mV indicated a channel more permeable to I^- than to Cl^-.

potential, the I^-/Cl^- permeability ratio can be calculated from the Goldman equation (equation 2). This ratio is 1.48, identifying Eisenman halide selectivity sequence I (Diamond and Wright, 1969). Accordingly, the type I Cl^- channel is an anion channel with the following permeability sequence: $I^->Br^->Cl^->F^-$. Although the net current at 0 mV clamp voltage and the reversal potential indicate a greater channel permeability to I^- than to Cl^-, the upward-curving shape of the *I*/*V* plot in Fig. 9 suggests that I^- blocks the channel, particularly at voltages that drive I^- into the channel from the cytoplasmic side.

When gluconate replaced Cl^- to produce a 46-fold Cl^- concentration difference across the patch membrane (Fig. 5B), the observed reversal potential of −80 to −90 mV falls slightly short of the Cl^- equilibrium potential (−97 mV), indicating a channel not ideally selective for Cl^-. When isethionate was used to replace Cl^-, the reversal potential shifted to values between −50 and −60 mV (*N*=3, data not shown). Thus, the type I channel is also permeable to isethionate and possibly to other organic anions.

Type II Cl^- channel: general characteristics

In addition to the type I Cl^- channel, some patches contained a second channel type that was also Cl^--permeable. The type II Cl^- channel had a lower conductance than the type I channel and a shorter open time and open probability. The type II Cl^- channel could not be studied in detail unless type I channels were absent or closed. Fig. 10 shows a representative current recording of two type II channels present in an excised apical membrane patch. The type II Cl^- channel exhibits rapid kinetics, with a mean open time of 7.54±1.46 ms and an open probability of 0.066±0.021 near 0 mV (means ± S.E.M., *N*=4).

The *I*/*V* plot of a type II Cl^- channel (Fig. 11) revealed no GHK rectification in the presence of a 46-fold Cl^- gradient from pipette to bath. Furthermore, the channel appeared to offer a small permeability to isethionate and gluconate. The permeability for both anions was similar, allowing us to pool the data from three separate experiments in which either isethionate or gluconate was used to replace Cl^- (Fig. 11). Channel conductance was 8 pS for the data shown in Fig. 11. Extrapolation of the *I*/*V* plot to zero current (dashed line) passes through the *x*-axis near −70 mV, falling short of the Cl^- equilibrium potential (−97 mV). This suggests that the type II Cl^- channel does not exhibit ideal permselectivity for Cl^-.

Since the type II channel was rarely observed in isolation from the type I channel and the small conductance and fast kinetics of this channel made measurements of current amplitude difficult, no further studies were attempted.

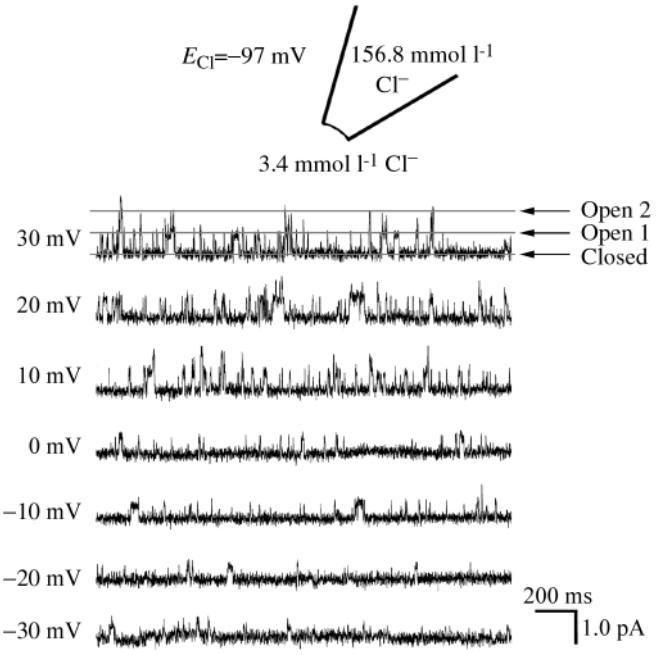

Fig. 10. Representative traces of the type II Cl^- channel at several clamp voltages. The patch was excised in the inside-out configuration with a 46-fold Cl^- gradient from pipette to bath (isethionate as the substitute anion). The patch contained two channels. Channel openings are shown as upward deflections in the current trace. Clamp voltages (V_c) are shown to the left of each trace. The data were filtered at 500 Hz. E_{Cl}, Cl^- equilibrium potential.

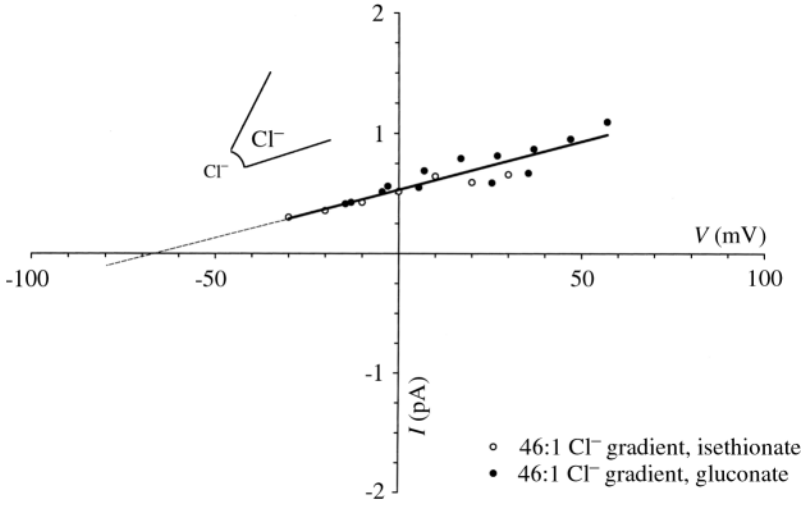

Fig. 11. Current/voltage (*I*/*V*) plot of the type II stellate cell Cl^- channel with control Ringer (156.8 mmol l^{-1} Cl^-) in the pipette and low-Cl^- Ringer (3.4 mmol l^{-1}) in the bath. Data from three patches were pooled; similar results were obtained using isethionate and gluconate as the substitute anion. The channel had a linear conductance of 8 pS. The extrapolated line (dashed) fell short of the equilibrium potential for Cl^- (–97 mV).

Discussion

In a previous study, we observed high channel densities in membrane patches excised from the luminal surface of Malpighian tubules of *Aedes aegypti* (Wright and Beyenbach, 1987). We found Cl^- channels with a single-channel conductance of 25 pS in approximately 10 % of the patches, but we could not be sure whether these channels came from principal or stellate cells.

With improved methods for dissecting Malpighian tubules, we were now able to expose the apical membrane of stellate cells and obtain patches from them. In view of the high channel density in these patches, pipettes with tip openings less than 0.5 μm^2 were needed to increase the likelihood of observing a single channel. Yet, in spite of these small pipette openings, we rarely observed single channels. The high channel density contributed to patches becoming noisy and unstable with clamp voltages greater than 30–40 mV on either side of zero. The cleanest recordings of channel activity were obtained at 0 mV clamp voltage, when a Cl^- concentration difference was the sole current source. To improve the signal-to-noise ratio of this diffusion-driven Cl^- current, we used a large Cl^- concentration difference (46-fold) across membrane patches. Moreover, we studied only excised membrane patches to be certain of electrochemical potentials for the identification of ion channels.

Although we occasionally observed cationic currents, anionic currents were the rule in apical membrane patches of stellate cells. These could be separated into a Cl^- channel of intermediate conductance and slow kinetics (type I) and a Cl^- channel of low conductance and fast kinetics (type II). The former was the principal object of attention in the present study.

Type I Cl^- channel and GHK rectification

The type I Cl^- channel exhibited Goldman–Hodgkin–Katz (GHK) rectification (Fig. 5), describing a situation in which channel conductance is dependent on the concentration of the permeating ion. Since the conductance of a solution depends on the concentration of ions, channel conductance is large for high concentrations and small for low concentrations. Furthermore, the conductance of, for example, a Cl^- channel is constant, and therefore linear (ohmic), when the Cl^- concentration on both sides of the channel is the same, a condition referred to as ‘symmetrical’ (Fig. 5A). In the case of asymmetric Cl^- concentrations, high on one side and low on the other, channel conductance becomes curvilinear as a function of concentration and voltage (Fig. 5B,C). Cl^- has a greater probability of entering the channel driven by a high Cl^- electrochemical potential than a low Cl^- potential. Accordingly, the channel conductance decreases as the electrochemical potential (and probability) for Cl^- entry decreases and asymptotically approaches the Cl^- equilibrium potential. This phenomenon is known as GHK rectification.

Two key assumptions in GHK rectification are (i) no interaction between diffusing ions, and (ii) a constant electric field across the channel (Hille, 1992). Since the experimental data obtained from the type I Cl^- channel can be closely fitted to a plot of the GHK current equation (equation 1; Fig. 5), the observed rectification stems primarily from the asymmetric Cl^- concentrations and not from the channel itself.

Outward Goldman rectification in the case $[Cl^-]_o<[Cl^-]_i$ is not a perfect inverse of inward rectification when $[Cl^-]_o>[Cl^-]_i$, suggesting additional mechanisms of rectification (Fig. 5). At 0 mV clamp voltage, the diffusion of Cl^- from a high Cl^- concentration in the patch pipette (extracellular side) to a low Cl^- concentration in the bath (intracellular side) carried 1.6 times the current carried in the opposite direction by the reversed Cl^- gradient. If the channel behaves in the intact stellate cell as it does in excised patches, it would favor absorptive rather than secretory Cl^- transport, which would not be expected from a transport pathway mediating transepithelial Cl^- secretion. Rectification can also result from the use of buffers and the presence of other large anions (Hanrahan and Tabcharani, 1990; Sheppard and Welsh, 1999; Tabcharani et al., 1997). Hence, additional studies are necessary to determine the mechanisms other than those producing GHK rectification.

Channel block by niflumic acid and DPC

Disulfonic stilbenes, such as SITS and DIDS, are large anions (1.3 nm) that block epithelial Cl^- channels from the extracellular side (Sheppard and Welsh, 1999). In contrast, the epithelial Cl^- channel known as CFTR (cystic fibrosis transmembrane conductance regulator) is blocked from the intracellular side by DIDS and 4,4′-dinitrostilbene-2,2′-disulfonic acid (DNDS) (Sheppard and Welsh, 1999). We found that 0.3 mmol l^{-1} DIDS or SITS was ineffective in blocking the type I channel from the intracellular side. Because of the difficulty in obtaining outside-out patches from these cells, we did not attempt studies of extracellular channel block by SITS and DIDS.

Niflumic acid, a blocker of Ca^{2+}-activated Cl^- channels, blocked the type I channel from the cytoplasmic side, but incompletely (Fig. 7B). In contrast, DPC blocked the type I channel completely, but the block was not entirely reversible after washout (Fig. 7C,D). Since DPC is a small molecule (0.3 nm), it may access binding sites deep in the channel, from where it is not readily dislodged, and it may be small enough to pass through the channel pore (Sheppard and Welsh, 1999). DPC could act as a 'permanent blocker', passing through the channel or, given its lipid permeability, passing through the membrane to reach its binding site (McCarty et al., 1993). Hence, washout of DPC from the *cis* side could leave DPC in the membrane or on the *trans* side, where it could block the channel, albeit with a lower effective concentration.

The type I Cl^- channel was also blocked by iodide, which is illustrated in Fig. 9 in which, at 0 mV clamp voltage, the net channel current is negative, consistent with the diffusion of I^- from the bath (cytoplasmic side) into the pipette. Increasing the clamp voltage to electronegative values (cytoplasmic side) was expected to increase the I^- current into the pipette. Instead, a decrease in net current is observed (Fig. 9). Thus, it seems that, in addition to permeating the channel, I^- can block it. Iodide behaves similarly in CFTR, leading to a wide range of I^-/Cl^- permeability ratios calculated for CFTR (Tabcharani et al., 1997). Even a low concentration of I^- (5 mmol l^{-1}) in the bathing solution can cause a voltage-dependent block of cell currents (Smith et al., 1999).

Activation and regulation of the type I Cl^- channel

It is possible that the type I stellate cell Cl^- channel is constitutively active in excised patches because excision of the membrane from the cell disrupts the normal regulatory mechanisms. Acute changes to the cytoskeleton expected from patch excision, the addition of cytochalasin (an actin-depolymerizing compound) or varying actin concentrations may modify the activation state of Cl^- channels, such as CFTR (Cantiello, 1996), Cl^- channels in renal proximal tubules (Suzuki et al., 1993) and volume-sensitive Cl^- channels (Shen et al., 1999). Thus, studies of the type I Cl^- channel in excised membrane patches may not reveal the normal functional properties of the channel in the intact cell.

It is widely accepted that the stimulation of transepithelial electrolyte secretion by leucokinin involves an increase in transepithelial Cl^- conductance mediated *via* an increase in intracellular Ca^{2+} concentration (Clark et al., 1998; O'Donnell and Spring, 2000; Yu and Beyenbach, 2000b). Ca^{2+} may activate Cl^- channels directly or indirectly, by first activating a protein kinase (Arreola et al., 1998; Begenisich and Melvin, 1998). Ca^{2+} may also affect the cytoskeleton and proteins associated with the constituents of intercellular junctions, thereby affecting paracellular Cl^- permeability (Yu and Beyenbach, 2000a). For these reasons, the effects of Ca^{2+} on the activity of the type I Cl^- channel in apical membrane patches of stellate cells were of interest.

The type I Cl^- channel was highly active in normal Ringer containing 1.7 mmol l^{-1} Ca^{2+} on the cytoplasmic side of the excised apical membrane patch (Figs 3, 4). Channel activity was undisturbed after removing Ca^{2+} from the cytoplasmic side by (i) removing Ca^{2+} from the Ringer's solution, and (ii) adding the strong Ca^{2+} chelator EGTA (Fig. 8). Ignoring Ca^{2+} concentrations on the cytoplasmic side of the patch, the type I channel is unlikely to mediate the Ca^{2+}-dependent effects of leucokinin, i.e. the 10-fold increase in transepithelial Cl^- conductance (Pannabecker et al., 1993). Nevertheless, the channel might still be Ca^{2+}-dependent, possibly *via* a Ca^{2+}-sensitive protein kinase that was lost with patch excision.

Type I Cl^- channel selectivity

In excised apical membrane patches of stellate cells, the I^-/Cl^- permeability ratio of type I Cl^- channel was 1.48, similar to the ratio measured for the tubule wall in microperfusion experiments (Yu and Beyenbach, 2000a). This ratio indicates Eisenman halide selectivity sequence I, in order of decreasing permeability: $I^->Br^->Cl^->F^->$isethionate. Since the tubule wall and type I Cl^- channels share the same halide selectivity sequence, the type I Cl^- channels may be part of the transepithelial pathway taken by Cl^- under control conditions. In contrast, when stimulated by leucokinin, the tubule wall exhibits Eisenman selectivity sequence III: $Br^->Cl^->I^->F^->$isethionate (Yu and Beyenbach, 2000a). Thus, leucokinin increases the transepithelial Cl^- conductance and increases the Cl^- selectivity of this conductive pathway (Pannabecker et al., 1993; Yu and Beyenbach, 2000a). Apart from amino acid substitutions that may change the ion selectivity of channels, we are not aware of ion channels changing permselectivity in response to primary or secondary messengers. Accordingly, the type I Cl^- channel appears not to be part of the transcellular pathway for Cl^- secretion under diuretic conditions triggered by leucokinin. To be sure, on-cell experiments testing the effects of leucokinin on the type I Cl^- channel are needed.

In addition to allowing the permeation of halides, the type I Cl^- channel permits the passage of organic anions. This conclusion is gleaned from reversal potentials when Cl^- was replaced on one side of the membrane patch with isethionate instead of gluconate. The channel offers a greater permeability to isethionate (two carbon atoms) than to gluconate (six carbon atoms), which is a frequent observation in studies of anion selectivity in epithelial cells (Boese et al., 1996; Gunther et al.,

1984; Rasola et al., 1992). Estimates of the molecular radii of gluconate and isethionate are 0.376 and 0.301 nm respectively (Smith et al., 1999). Large anions and osmolytes such as sorbitol, taurine and betaine are also known to pass through some Cl^- channels (Begenisich and Melvin, 1998). Permeability to organic anions and a weak selectivity for Cl^- (Eisenman sequence I) are characteristics of volume-sensitive Cl^-/anion channels (Begenisich and Melvin, 1998). Thus, the type I channel may play a role in cell volume regulation.

Cl⁻ channels in Drosophila melanogaster *and* Aedes aegypti *Malpighian tubules*

O'Donnell et al. (1998) have found a maxi-Cl^- channel with a conductance of 256 pS and fast kinetics in membrane patches of the luminal surface of *Drosophila melanogaster* Malpighian tubules. Vibrating probe studies of transepithelial current sinks suggest that the maxi-Cl^- channel is located in stellate cells, where it is thought to mediate transepithelial secretion of Cl^- during stimulation with leucokinin (O'Donnell et al., 1998).

In the present study, we examined the apical membranes of stellate cells of *Aedes aegypti* Malpighian tubules under control conditions; the effect of leucokinin on channel activity was not studied. A maxi-Cl^- channel was never observed. Instead, Cl^- channels of moderate and low conductance were observed. The high density of type I Cl^- channels suggests a possible role in transepithelial Cl^- secretion under control conditions, mediating the transport of Cl^- from the cell into the tubule lumen. To link this channel definitively to transepithelial Cl^- secretion, thereby proving a transcellular route for Cl^- secretion, the mechanism and driving force of Cl^- entry across the basolateral membrane of stellate cells must be elucidated.

We thank Dr Larry Stoner (SUNY Health Science Center, Syracuse, NY, USA) for the introduction to computer-assisted analysis of patch-clamp data, Shannon Caldwell and Dr Mandayam Parthasarathy (Cornell Integrated Microscopy Center) for the electron micrographs, Dr Linda Nowak, Dr Mark Baustian, Ricard Masia and Ming-Jiun Yu for discussions and insights and the National Science Foundation for enabling this study under grants IBN 9604394 and IBN 0078058.

References

Arreola, J., Melvin, J. E. and Begenisich, T. (1998). Differences in regulation of Ca^{2+}-activated Cl^- channels in colonic and parotid secretory cells. *Am. J. Physiol.* **274**, C161–C166.

Begenisich, T. and Melvin, J. E. (1998). Regulation of chloride channels in secretory epithelia. *J. Membr. Biol.* **163**, 77–85.

Beyenbach, K. W. (1994). Mechanism and regulation of electrolyte transport in Malpighian tubules. *J. Insect Physiol.* **41**, 197–207.

Beyenbach, K. W., Aneshansley, D. J., Pannabecker, T. L., Masia, R., Gray, D. and Yu, M.-J. (2000). Oscillations of voltage and resistance in Malpighian tubules of *Aedes aegypti*. *J. Insect Physiol.* **46**, 321–333.

Beyenbach, K. W. and Petzel, D. H. (1987). Diuresis in mosquitoes: role of a natriuretic factor. *News Physiol. Sci.* **2**, 171–175.

Boese, S. H., Wehner, F. and Kinne, R. K. (1996). Taurine permeation through swelling-activated anion conductance in rat IMCD cells in primary culture. *Am. J. Physiol.* **271**, F498–F507.

Cantiello, H. F. (1996). Role of the actin cytoskeleton in the regulation of the cystic fibrosis transmembrane conductance regulator. *Exp. Physiol.* **81**, 505–514.

Clark, T. M., Hayes, T. K., Holman, G. M. and Beyenbach, K. W. (1998). The concentration-dependence of CRF-like diuretic peptide: mechanisms of action. *J. Exp. Biol.* **201**, 1753–1762.

Diamond, J. M. and Wright, E. M. (1969). Biological membranes: the physical basis of ion and nonelectrolyte selectivity. *Annu. Rev. Physiol.* **31**, 581–646.

Gunther, R. D., Schell, R. E. and Wright, E. M. (1984). Ion permeability of rabbit intestinal brush border membrane vesicles. *J. Membr. Biol.* **78**, 119–127.

Hanrahan, J. W. and Tabcharani, J. A. (1990). Inhibition of an outwardly rectifying anion channel by Hepes and related buffers. *J. Membr. Biol.* **116**, 65–77.

Hayslett, J. P., Goegelein, H., Kunzelmann, K. and Greger, R. (1987). Characteristics of apical chloride channels in human colon cells (HT29). *Pflügers Arch.* **410**, 487–494.

Hille, B. (1992). *Ionic Channels of Excitable Membranes*, pp. 341–347. Sunderland, MA: Sinauer Associates Inc.

Juan, J. L. and Carlson, S. D. (1994). Analog of vertebrate anionic sites in blood–brain interface of larval *Drosophila*. *Cell Tissue Res.* **277**, 87–95.

McCarty, N. A., McDonough, S., Cohen, B. N., Riordan, J. R., Davidson, N. and Lester, H. A. (1993). Voltage-dependent block of the cystic fibrosis transmembrane conductance regulator Cl^- channel by two closely related arylaminobenzoates. *J. Gen. Physiol.* **102**, 1–23.

O'Donnell, M. J., Dow, J. A. T., Huesmann, G. R., Tublitz, N. J. and Maddrell, S. H. P. (1996). Separate control of anion and cation transport in Malpighian tubules of *Drosophila melanogaster*. *J. Exp. Biol.* **199**, 1163–1175.

O'Donnell, M. J., Rheault, M. R., Davies, S. A., Rosay, P., Harvey, B. J., Maddrell, S. H., Kaiser, K. and Dow, J. A. (1998). Hormonally controlled chloride movement across *Drosophila* tubules is *via* ion channels in stellate cells. *Am. J. Physiol.* **274**, R1039–R1049.

O'Donnell, M. J. and Spring, J. H. (2000). Modes of control of insect Malpighian tubules: synergism, antagonism, cooperation and autonomous regulation. *J. Insect Physiol.* **46**, 107–117.

Pannabecker, T. L., Hayes, T. K. and Beyenbach, K. W. (1993). Regulation of epithelial shunt conductance by the peptide leucokinin. *J. Membr. Biol.* **132**, 63–76.

Rasola, A., Galietta, L. J., Gruenert, D. C. and Romeo, G. (1992). Ionic selectivity of volume-sensitive currents in human epithelial cells. *Biochim. Biophys. Acta* **1139**, 319–323.

Satmary, W. M. and Bradley, T. J. (1983). The distribution of cell types in the Malpighian tubules of *Aedes taeniorhynchus*. *Int. J. Insect Morph. Embryol.* **13**, 209–214.

Shen, M. R., Chou, C. Y., Hsu, K. F., Hsu, K. S. and Wu, M. L. (1999). Modulation of volume-sensitive Cl^- channels and cell volume by actin filaments and microtubules in human cervical cancer HT-3 cells. *Acta Physiol. Scand.* **167**, 215–225.

Sheppard, D. N. and Welsh, M. J. (1999). Structure and function of the CFTR chloride channel. *Physiol. Rev.* **79**, S23–S45.

Smith, S. S., Steinle, E. D., Meyerhoff, M. E. and Dawson, D. C. (1999). Cystic fibrosis transmembrane conductance regulator. Physical basis for lyotropic anion selectivity patterns. *J. Gen. Physiol.* **114**, 799–818.

Suzuki, M., Miyazaki, K., Ikeda, M., Kawaguchi, Y. and Sakai, O. (1993). F-actin network may regulate a Cl^- channel in renal proximal tubule cells. *J. Membr. Biol.* **134**, 31–39.

Tabcharani, J. A., Linsdell, P. and Hanrahan, J. W. (1997). Halide permeation in wild-type and mutant cystic fibrosis transmembrane conductance regulator chloride channels. *J. Gen. Physiol.* **110**, 341–354.

Wright, J. M. and Beyenbach, K. W. (1987). Chloride channels in apical membranes of mosquito Malpighian tubules. *Fedn. Proc.* **46**, 1270 (Abstract).

Yu, M.-J. and Beyenbach, K. W. (2000a). Leucokinin and the modulation of the shunt pathway in Malpighian tubules. *J. Insect Physiol.* (in press).

Yu, M.-J. and Beyenbach, K. W. (2000b). Leucokinin-VIII increases epithelial shunt conductance *via* a receptor-mediated pathway involving calcium. *FASEB J.* **14**, A579 (Abstract).